Materials Science & Engineering B 261 (2020) 114772

Contents lists available at ScienceDirect

Materials Science & Engineering B

journal homepage: www.elsevier.com/locate/mseb

Preparation of spintronically active ferromagnetic contacts based on Fe, Co and Ni Graphene nanosheets for Spin-Field Effect Transistor

Neetu Gyanchandani[a], Santosh Pawar[b], Prashant Maheshwary[a], Kailash Nemade[c,*]

[a] JD College of Engineering and Management, Nagpur 441501, India
[b] School of Engineering, Dr. A.P.J. Abdul Kalam University, Indore 452016, India
[c] Department of Physics, Indira Mahavidyalaya, Kalamb 445401, India

ARTICLE INFO

Keywords:
Ferromagnetic contacts
Spintronics
Graphene
Spin field effect transistor

ABSTRACT

Present experimentation reports the interaction between graphene and transition Metal (Fe, Co and Ni), in the context of ferromagnetism. Fe-Graphene, Co-Graphene and Ni-Graphene samples were prepared by simple ex-situ approach followed by probe-sonication technique. The prepared samples were characterized by X-ray diffraction (XRD) technique and Scanning Electron Microscope (SEM) analysis. To study magnetic properties of prepared samples, few tests were performed namely Vibrating Sample Magnetometer (VSM) technique, Magnetoconductance Study, Temperature-dependent Magnetization Measurements and Large positive Magnetoresistance Study. Results obtained were analyzed specially in the context of Spin-Field Effect Transistor (s-FET) application.

1. Introduction

In scientific community, graphene is well accepted class of material which has important features as light weight, good transport properties and ease of synthesis. Spintronics is rapidly emerging area of research, which deals with the use of electron spin degree of freedom instead of/ in addition to electrical charge of electron. However, spin-polarization is very important condition for spintronics application which can easily be achieved by using ferromagnetic materials. The transition metals Fe ($3d^6s^2$), Co ($3d^7s^2$) and Ni ($3d^8s^2$) are partially filled d-block element and also well-known ferromagnets at room temperature. In metal spin relaxation time and length is very short, whereas it is long in semiconductors [1].

Graphene-based spintronics is comparatively a new field of research and development. Recently, scientific community has seen noteworthy progress in spintronics technology. The graphene-based materials are the potential category of materials for spintronics application for the reasons mentioned below,

- Graphene based magnetic materials have long spin lifetime and diffusion length [2].
- Graphene is a very promising spin channel material, as it shows room temperature spin transport with long spin diffusion lengths up to several micrometers [3].
- Graphene has special motivating physical property i.e. tunable carrier concentration and high electronic mobility through Gate Voltage [4].
- Graphene has high electron mobility (about ten times higher) compared to commercial silicon wafers. It has long spin-relaxation length and ballistic transport characteristics (electrons can travel 300 nm or more without scattering) [5–9].
- Above characteristics of graphene facilitates huge scope to develop the spin-polarized devices, mainly spin-Field Effect Transistors. Therefore, scientists have concentrated on developing efficient magnetically active graphene based spintronics materials. Use of graphene based ferromagnetic materials for spintronics application needs an insight about the behavior of magnetic properties at the interfaces of graphene and Fe, Co and Ni nanocrystallite [10–12].

Therefore, in this primary research attempt of magnetic behavior of Fe, Co and Ni loaded Graphene nanosheets has been studied for future spintronics applications specially Spin-Field Effect Transistors. With this in mind, different tests as Vibrating Sample Magnetometer (VSM) Measurements, Magnetoconductance Study, Temperature dependent Magnetization Measurements, Large positive Magnetoresistance Study were performed and their results were studied to understand the ferromagnetic behavior of samples (Fe, Co, Ni – Graphene) for spintronics application.

* Corresponding author.
E-mail address: krnemade@gmail.com (K. Nemade).

https://doi.org/10.1016/j.mseb.2020.114772
Received 27 March 2020; Received in revised form 1 June 2020; Accepted 1 September 2020

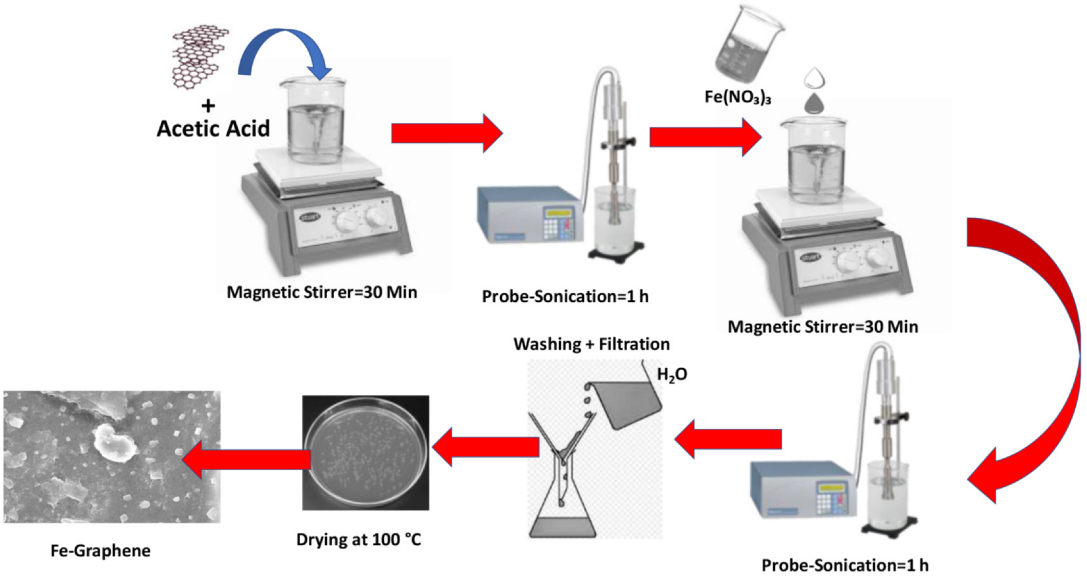

Fig. 1. Schematic synthesis process of Fe-Graphene nanosheets.

2. Experimentation

2.1. Synthesis of (Fe, Co & Ni-Graphene) nanosheets

Fig. 1 depicts the synthesis procedure of (Fe, Co & Ni-Graphene) nanosheets. Graphene used in this work is obtained by using previously reported method [13]. Firstly, to synthesize Fe-Graphene, 50 g of graphene sheets were dissolved in 100 ml acetic acid under magnetic stirring for 30 min. Secondly, the suspension of Fe-Graphene and acetic acid was subjected to probe-sonication for 1 h. Thirdly, 0.5 mg of Fe $(NO_3)_3$ was dissolved in 10 ml of acetic acid, which was added in former solution drop by drop under constant magnetic stirring for 30 min. The resultant suspension then was subjected to probe-sonication for 1 h. The final solution was then filtered and washed several times by deionized water to remove the impurities. Finally, black colored precipitate was collected and dried at 100 °C in oven.

The same procedure was adopted for the preparation of Co-Graphene and Ni-Graphene using precursors $Co(NO_3)_2$ and $Ni(NO_3)_2$, respectively. The schematic synthesis process of Fe-Graphene nanosheets shown in Fig. 1. Temperature conditioning was employed to all the three final products to form homogeneous magnetic system. The final product of all three samples were kept for heating in the temperature range of 100–500 °C in stepwise manner with an interval of 100 °C. At each fixed value of temperature, sample was heated for 60 min. Similarly, the sample was allowed to cool at 400, 300, 200 and 100 °C each for 60 min.

2.2. Characterization methods

The structural study of Fe-Graphene, Co-Graphene and Ni-Graphene nanosheets were executed using X-ray diffraction (XRD) analysis with Rigaku Miniflex XRD set up CuKα radiation (λ = 1.5406 Å). Transmission electron microscopy with selected area diffraction pattern analysis was captured using TEM-Tecnai F-30107; Philips. The surface topography of Fe-Graphene, Co-Graphene and Ni-Graphene nanosheets was investigated by field emission scanning electron microscopy (FESEM) by using Scanning Electron Microscopy instrument, Model: ZEISS SIGMA operating at 5 kV ETH voltage. In addition to XRD and SEM analysis, elemental composition analysis was performed by using an energy dispersive X-ray analysis (EDAX) instrument, Model: EAG AN461.

To explore the ferromagnetic behavior of Fe-Graphene, Co-Graphene and Ni-Graphene nanosheets, Vibrating Sample Magnetometer (VSM) technique was employed at room temperature using VSM set up (Quantum Design Model- PAR 155) having specifications as Range: 0.00001 to 10,000 emu and Magnetic field: −10 to +10 kOe. To study ferromagnetic behavior in detail, the temperature dependent magnetization measurements with zero field cooled (ZFC) and field cooled (FC) condition were performed at 1000 Oe magnetic field strength using special Vibrating Sample Magnetometer (Lake Shore-7410) with temperature range −4.2 K to 1273 K. In the magnetoconductance measurement process, the material under study was mounted in cryostat-Janis CCS-350s, which was positioned between the pole pieces of an electromagnet (Lakeshore EM647). The magnetic field with the maximum strength of 20 kOe was applied and measured by Gauss Meter, Lakeshore 421 kept close to the material. The current–voltage characteristics was measured by a Keithley 2400 Source Meter and used further for the calculation of magnetoconductance.

Using Hall measurements, transport properties of samples were determined. The magnetoresistance (MR) was measured using direct current (Van der Pau method) at room temperature in the magnetic fields at around 0.5 T. For MR measurement, thin films of samples were prepared using spin coating technique with thickness ranging between 268 and 285 nm. MR is defined as, MR (%) = $[(R_B - R_0)/R_0] \times 100$ where R_0 is the initial sample resistance and R_B is its resistance in the magnetic field.

3. Results and discussion

3.1. Structural and morphological study of graphene

Fig. 2(a) depicts the XRD pattern of graphene, which comprises the signature peaks of graphene at 26.3° and 44.2° corresponds to plans (002) and (100), respectively. Whereas the inset of figure shows the Raman spectra of graphene. This spectrum also comprises the characteristics bands of graphene, D band (~1300 cm^{-1}), G band (~1580 cm^{-1}), and 2D band (~2720 cm^{-1}) [14]. Fig. 2(b) shows the TEM image of pure graphene with selected area diffraction pattern (inset). Inset shows a well-defined hexagonal array indicating structural purity of planes in graphene and also indicates graphene does not have a large number of sheets. The XRD, Raman and TEM analysis of graphene obtained in present study has structural purity.

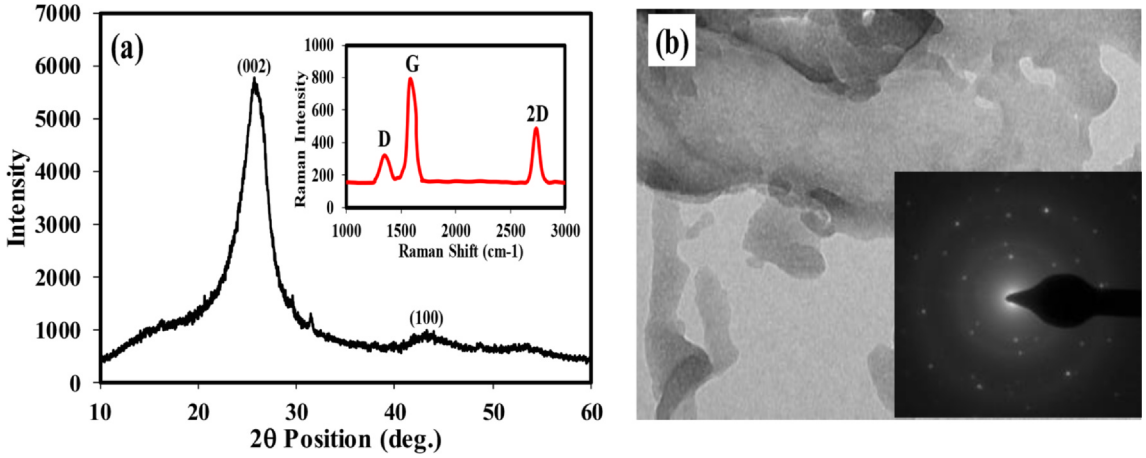

Fig. 2. (a) XRD pattern of pristine graphene. Inset of image shows Raman spectra of graphene. (b) TEM image of graphene and inset displays selected area diffraction pattern.

3.2. XRD analysis of composites

Fig. 3(a–c) shows the XRD pattern of Fe-Graphene, Co-Graphene and Ni-Graphene nanosheets, respectively. All three XRD patterns comprise two broad peaks, (0 0 2) and (1 0 0), which are signature peaks of graphene at 2θ positions of 26.3° and 44.2°. The corresponding peaks of graphene are in good agreement with recently reported work in literature [15,16]. No significant peak appears for the Fe, Co and Ni, which indicates that the orientation of graphene layers is not greatly influenced by nanocrystallites Fe, Co and Ni. The discernible peak at 26.42° in XRD of Fe-graphene composite as shoulder peak is the indication of formation of iron oxide nano-island. The previous report of Narayanaswamy et al demonstrated that the oxidation behavior of Fe can be controlled by the concentration of graphene in composite [17].

3.3. SEM study

Fig. 4(a–c) shows the SEM images and elemental X-ray mapping of (a) Fe-Graphene (b) Co-Graphene and (c) Ni-Graphene. The SEM image confirms that nanocrystallites Fe, Co and Ni are uniformly distributed over the graphene surface. No significant agglomeration observed in SEM micrographs. The elemental analysis was done using EDAX

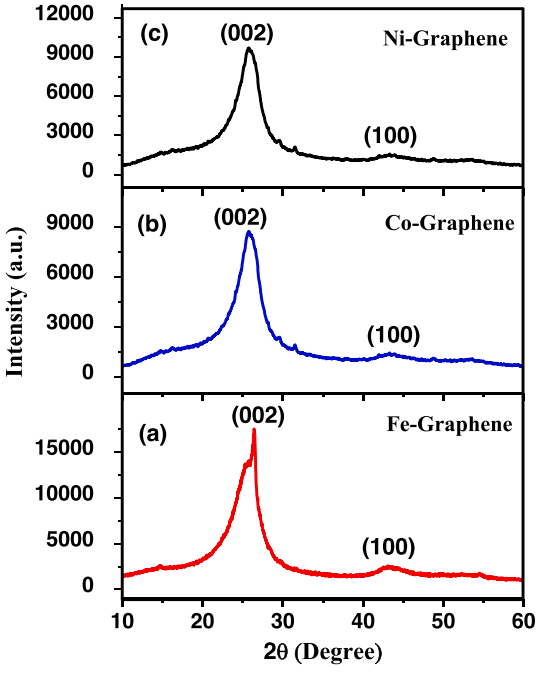

Fig. 3. XRD patterns of (a) Fe-Graphene, (b) Co-Graphene and (b) Ni-Graphene.

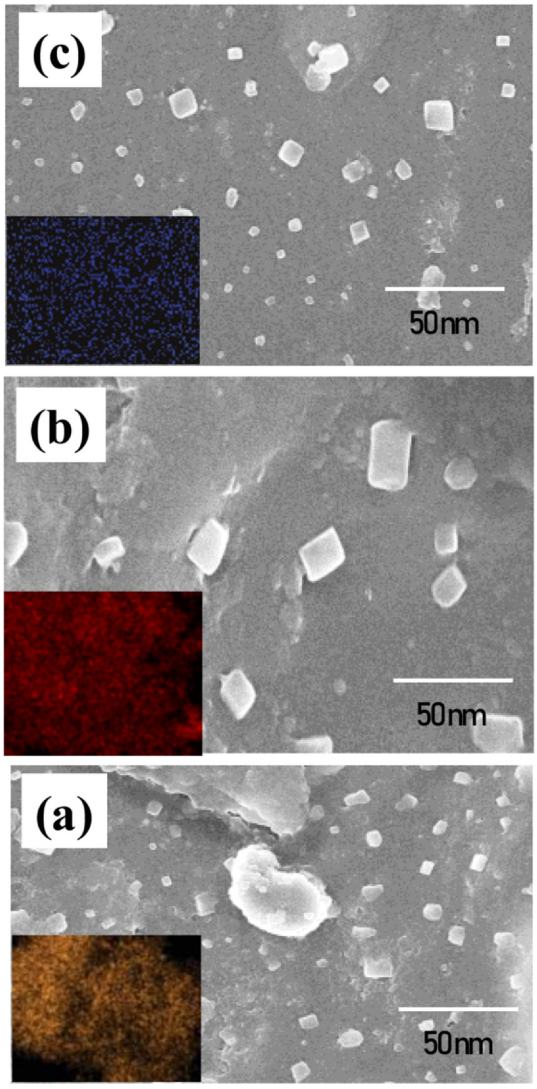

Fig. 4. SEM images and elemental X-ray mapping of (a) Fe-Graphene (b) Co-Graphene and (c) Ni-Graphene.

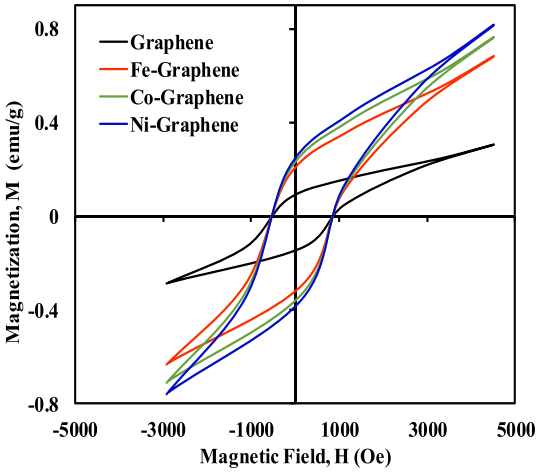

Fig. 5. VSM hysteresis loop of Fe-Graphene, Co-Graphene and Ni-Graphene nanosheets.

spectroscopy. The elemental analysis also confirms that nanocrystallites Fe, Co and Ni are distributed over the graphene surface. In present work, as the Fe, Co and Ni nanoparticles adsorbed by graphene results in formation of an electron transport channel between Fe, Co and Ni nanoparticles and graphene. In this type of materials, electron mobility proportional to surface electron concentration and the diameter of adsorbed atoms [18].

3.4. Magnetic characteristics

3.4.1. Vibrating sample magnetometer (VSM) measurements

Theoretically, the pristine graphene is diamagnetic in nature due to sp^2 hybridization. In the present study, obtained graphene synthesized using electrochemical exfoliation of graphite, which definitely comprises some defects, which imprint magnetic features into graphene [19]. Therefore, graphene used in present study shows weaken magnetic behavior. Fig. 5 shows the hysteresis loops of pristine graphene, Fe-Graphene, Co-Graphene and Ni-Graphene nanosheets, which were obtained at room temperature (298 K). The well-defined hysteresis curves indicate that good ferromagnetic ordering with considerably large coercivity was observed in Fe-Graphene, Co-Graphene and Ni-Graphene nanosheets. The values of coercivity, remanant magnetization and saturation magnetization estimated from hysteresis loops are presented in Table 1.

Fig. 4 and the values of coercivity (Hc), remanant magnetization (Mr) and saturation magnetization (Ms) listed in Table 1 for Fe-Graphene, Co-Graphene and Ni-Graphene nanosheets clearly indicates that synthesized materials exhibit ferromagnetic behavior. Actually, the presence of intrinsic magnetism in sp2 hybridized pure graphene has been a controversial topic [20]. In literature, few reports show that graphene exhibit uncommon magnetic properties including spin glass and magnetic switching application due the edge states arising from the nonbonding electrons [21,22]. The origin of magnetism in pristine graphene comes only due to the local states introduced by defects and molecular adsorption [23,24]. Kaur et al [25] and Wang et al. [26] studied that graphene may become magnetically active by removing the functional groups like −OH, −COOH, −O− and −C═O, which introduce the point defects and extended defects. In this way, graphene may become magnetically active.

Table 1
The measurement of coercivity (Hc), remanant magnetization (Mr) and saturation magnetization (Ms) of (a) Fe-Graphene, (b) Co-Graphene and (c) Ni-Graphene nanosheets.

Sample	Hc (Gauss)	Mr (emu/gm)	Ms (emu/gm)
Pristine Graphene	540	0.0754	0.306
Fe-Graphene	535	0.2002	0.682
Co-Graphene	537	0.2002	0.761
Ni-Graphene	534	0.2010	0.816

The presence of ferromagnetic behavior in nanosheets assigned to creation of more defective sites in graphene sheets due to addition of Fe, Co and Ni nanocrystallites. Due to the presence of Fe, Co and Ni clusters, nanosheets may exhibit the strong exchange interaction with ions and result in ferromagnetism. Abtew et al. [27] shows that spatial overlap, energy and symmetry matching between transition metals-dz^2 and C-pz orbitals results in good magnetic characteristics. In addition, the work of Abtew et al and co-worker demonstrated that charge transfer of 0.05e per C atom from Co to graphene and 0.07e per C atom from Ni to graphene induced ferromagnetism in graphene sheets.

The gradual increase in the values of remanant magnetization, saturation magnetization and area under the hysteresis loop of Fe-Graphene, Co-Graphene and Ni-Graphene nanosheets, clearly indicate that the ferromagnetism observed in samples was largely due to the outcome of charge transfer from Fe, Co and Ni to graphene and small due to intrinsic defects present in the graphene [28].

3.4.2. Magnetoconductance study

Fig. 6 depicts the magnetoconductance curve of Fe-Graphene, Co-Graphene and Ni-Graphene nanosheets as a function of the magnetic field at room temperature (298 K). The magnetoconductance is very important tool to identify microscopic behavior of ferromagnetic system. This parameter is used to identify the scattering centers present in the sample [28]. The magnetoconductance shows positive value on entire scale of magnetic field at room temperature (298 K). The magnetoconductance in Fe-Graphene, Co-Graphene and Ni-Graphene nanosheets is attributed to weak spin-orbit coupling. The magnetoconductance curve does not comprise any peak in low magnetic field [29,30], which indicates that the contribution of intrinsic impurities or defects present in the graphene in magnetoconductance are negligible. In this case, it is due to the interaction between conduction electrons and potential barrier at the graphene and Fe, Co, Ni interface. The magnetoconductance curve with no peak is an indication of good quality interface formed between graphene and Fe, Co, Ni nanocrystallite. As the concentration of Fe, Co, Ni nanocrystallite in graphene is very less, magnetoconduction has happened through graphene.

3.4.3. Temperature dependent magnetization Measurements

Fig. 7(a–c) depicts the temperature dependent magnetization data recorded under zero field cooled (ZFC) and field cooled (FC) conditions

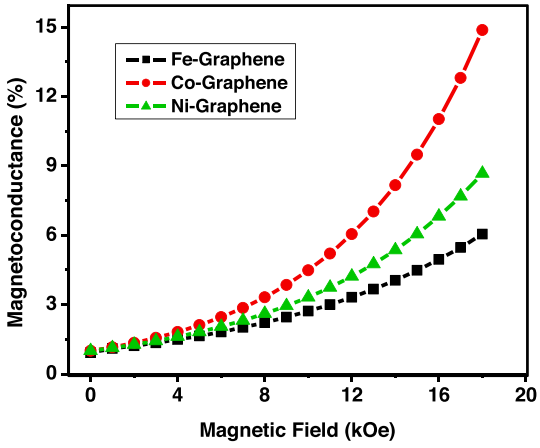

Fig. 6. Magnetoconductance curve of Fe-Graphene, Co-Graphene and Ni-Graphene nanosheets as a function of magnetic field at room temperature (298 K).

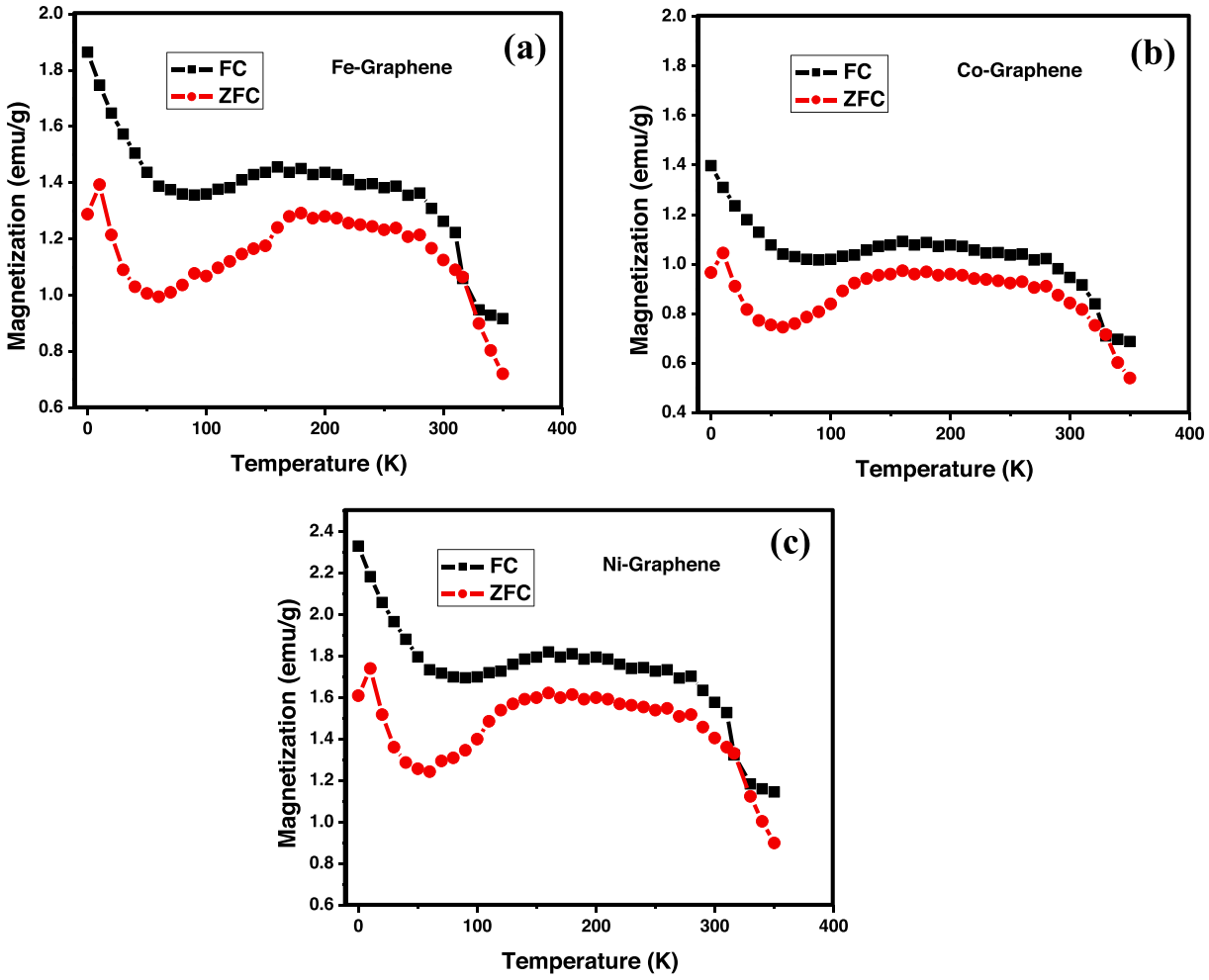

Fig. 7. Magnetization (Ms) as a function of temperature (a) Fe-Graphene, (b) Co-Graphene and (c) Ni-Graphene nanosheets measured under zero field cooled (ZFC) and field cooled (FC) condition under 1000 Oe magnetic field strength.

for external magnetic field 1000 Oe in the temperature range of 2–350 K for Fe-Graphene, Co-Graphene and Ni-Graphene nanosheets, respectively. In case of ZFC curve, Fe-Graphene, Co-Graphene and Ni-Graphene nanosheets show magnetization peaks at around 10 K. After 300 K, magnetization gradually drops up to 350 K. Similarly, FC curve shows no peak around 10 K with higher value of magnetization. The FC curve also shows gradual decrease in magnetization after 300 K. The slight difference in ZFC and FC data over the temperature range may be ascribed to the existence of small amount of magnetic inhomogeneous phase in prepared samples [31]. This type of behavior of samples is useful in spintronics and spin-glass application [32–35].

3.4.4. Large positive magnetoresistance study

Fig. 8 displays the magnetoresistance (MR) of Fe-Graphene, Co-Graphene and Ni-Graphene nanosheets versus magnetic field at a room temperature (298 K). The maximum value of MR around 94.87% was associated with Fe-Graphene sample, whereas minimum value of MR was 61.43% for Co-Graphene sample. All the measured MR values were positive, having quadratic magnetic field dependence behavior up to 0.05 T. Further, the MR values shows nearly linear dependence in the fields up to 0.5 T. The higher value of MR in Fe-Graphene sample is attributed to the process of hydrolysis of ferric nitrate, which produces islands of iron hydroxide and iron oxide on graphene surface [36]. These islands influenced the transport properties of graphene, similar to nanodiamonds work on graphene surface. These islands on graphene follow sp^3 configuration, which significantly alters the conductivity of sample [37]. In the present work, we conclude that ex-situ approach of

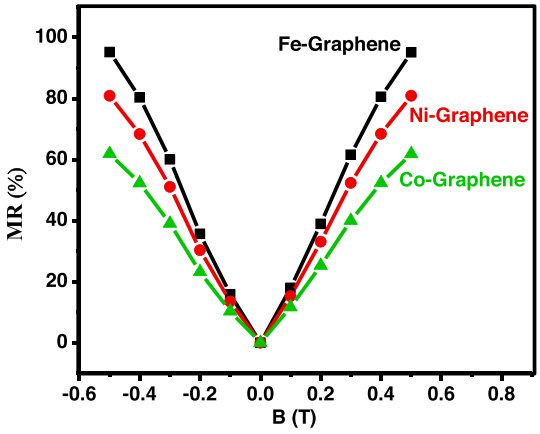

Fig. 8. The MR (%) of Fe-Graphene, Co-Graphene and Ni-Graphene nanosheets versus magnetic field at a room temperature.

Fe-Graphene, Co-Graphene and Ni-Graphene composite preparation create the islands of respective metal hydroxide and their oxide. Presently, we confirmed it from TEM and SEM images of pure graphene and composite. The comparative study of different ferromagnetic materials presented in Table 2, which are suitable for spintronic applications reported in the literature.

In the light of above discussion, it is observed that Co-Graphene is quite good material as ferromagnetic contacts in Spin-Field Effect

Table 2
Comparative study of different ferromagnetic materials, suitable for spintronic applications reported in the literature with regard to MR ratio.

Sample	Resistance type	Magneto-resistance	Ref.
α-Fe_2O_3 decorated graphene	Negative	32%	[38]
Graphene Oxide-Iron Oxide Nanocomposite	Positive	280%	[39]
Graphite intercalated with cobalt	Positive	148%	[40]
Co cluster decorated graphene	Negative	10%	[41]
Multilayer Graphene Grown on Nickel	Negative	10000%	[42]
Ni/graphene/Ni junctions	Positive	0.1%	[43]
Fe-Graphene	Positive	94.87%	This work
Co-Graphene	Positive	61.80%	This work
Ni-Graphene	Positive	80.89%	This work

Transistor (s-FET) application. Because, the origin of ferromagnetism between graphene and Co is due to electronic structure modifications. The US patent designed and published by Kelber et al shows that the charge current induces a spin current in the graphene, and it can be measured easily using spin selective cobalt electrodes. This work accomplishes that Graphene deposited over the Cobalt acts like efficient source and drain in field effect transistor. The fabricated spin- field effect transistor device shows durability, low power consumption, rapid switching action at room temperature [44].

In s-FET following three processes are extremely important,

Injection of spin polarized current of electron through the 2-dimentional electron gas channel from FM contacts (Source).
Transport of electrons through 2-dimentional electron gas channel without losing the spin direction
Detection of spin polarized current into FM contact (Drain).

In the working of s-FET, first and third process purely depends on quality of ferromagnetic materials, as it is used as ferromagnetic contacts (Source and Drain) in s-FET application. The 2-dimentional electron gas channel is heavily doped n-type silicon wafer, it has good compatibility with magnetically active Co-Graphene ferromagnetic material.

4. Conclusions

In summary, Fe, Co and Ni loaded Graphene explores the induced magnetism due to the charge transfer effect between graphene and Fe, Co, Ni interfaces. The VSM measurement shows that coercivity, remanant magnetization and saturation magnetization of Fe-Graphene, Co-Graphene and Ni-Graphene nanosheets show significant enhancement over the pure graphene. The magnetoconductance study discloses that the contribution of intrinsic impurities or defects present in the graphene in magnetoconductance is negligible. The ZFC and FC data shows that the small amount of magnetic inhomogeneous phase is present in prepared samples, which is useful in spintronics and spin-glass application. All samples show positive magnetoresistance having quadratic magnetic field dependence behavior up to 0.05 T and then linear dependence in the fields up to 0.5 T. The study reveals that Co-Graphene is quite good ferromagnetic material as Source and Drain contact application in s-FET.

Declaration of Competing Interest

The authors declare that they have no known competing financial interests or personal relationships that could have appeared to influence the work reported in this paper.

Acknowledgments

Prof. (Mrs.) Neetu Gyanchandani is very much thankful to Dr. S.R. Choudhary, Principal, JD College of Engineering and Management, Nagpur for providing necessary academic help.

Data availability

The raw/processed data required to reproduce these findings cannot be shared at this time as the data also forms part of an ongoing study.

References

[1] V. Shukla, Observation of critical magnetic behavior in 2D carbon-based composites, Nanoscale Adv. 2 (2020) 962–990.
[2] W. Han, K. Pi, K.M. McCreary, Y. Li, J.J.I. Wong, A.G. Swartz, R.K. Kawakami, Tunneling Spin Injection into Single Layer Graphene, Phys. Rev. Lett. 105 (2010) 167202.
[3] N. Tombros, C. Jozsa, M. Popinciuc, H.T. Jonkman, B.J. van Wees, Electronic spin transport and spin precession in single graphene layers at room temperature, Nature 448 (2007) 571–574.
[4] S.D. Sarma, S. Adam, E.H. Hwang, E. Rossi, Electronic transport in two-dimensional graphene, Rev. Mod. Phys. 83 (2011) 407.
[5] A.K. Geim, K.S. Novoselov, The rise of graphene, Nat. Mater. 6 (2007) 183–191.
[6] K.S. Novoselov, Z. Jiang, Y. Zhang, S.V. Morozov, H.L. Stormer, U. Zeitler, J.C. Maan, G.S. Boebinger, P. Kim, A.K. Geim, Science 315 (2007) 1379.
[7] K.S. Novoselov, A.K. Geim, S.V. Morozov, D. Jiang, M.I. Katsnelson, I.V. Grigorieva, S.V. Dubonos, A.A. Firsov, Two-dimensional gas of massless Dirac fermions in graphene, Nature 438 (2005) 197–200.
[8] P.B. Neetu Gyanchandani, P. Maheshwary, N. Nagrale, K. Indurkar, K.R.N. Jagane, Recent advancements in the field of ballistic and non-ballistic spin-based field-effect transistors, AIP Conf. Proc. 2104 (2019) 020018.
[9] T. Ohta, A. Bostwick, T. Seyller, K. Horn, E. Rotenberg, Controlling the electronic structure of bilayer graphene, Science 313 (2006) 951–954.
[10] Y.S. Dedkov, M. Fonin, C. Laubschat, A possible source of spin-polarized electrons: The inert graphene/Ni(111) system, Appl. Phys. Lett. 92 (2008) 052506.
[11] Y.S. Dedkov, M. Fonin, Electronic and magnetic properties of the graphene–ferromagnet interface, New J. Phys. 12 (2010) 125004.
[12] Y. Murata, V. Petrova, B.B. Kappes, A. Ebnonnasir, I. Petrov, Y.-H. Xie, C.V. Ciobanu, S. Kodambaka, Moire superstructures of graphene on faceted nickel islands, ACS Nano 4 (2010) 6509–6514.
[13] K.R. Nemade, S.A. Waghuley, Chemiresistive gas sensing by few-layered graphene, J. Electron. Mater. 42 (2013) 2857–2866.
[14] Z. Ni, Y. Wang, T. Yu, Z. Shen, Raman spectroscopy and imaging of graphene, Nano Res. 1 (2008) 273–291.
[15] X. Wang, L. Zhang, Green and facile production of high-quality graphene from graphite by the combination of hydroxyl radicals and electrical exfoliation in different electrolyte systems, RSC Adv. 9 (2019) 3693–3703.
[16] Y. Zhao, S. Chen, B. Sun, D. Su, X. Huang, H. Liu, Y. Yan, K. Sun, G. Wang, Graphene Co3O4 nanocomposite as electrocatalyst with high performance for oxygen evolution reaction, Sci. Rep. 5 (2015) 7629.
[17] V. Narayanaswamy, I.M. Obaidat, A.S. Kamzin, S. Latiyan, S. Jain, H. Kumar, C. Srivastava, S. Alaabed, B. Issa, Synthesis of graphene oxide-Fe3O4 based nanocomposites using the mechanochemical method and in vitro magnetic hyperthermia, Int. J. Mol. Sci. 20 (2019) 3368–3371.
[18] X. Fang, X. Yu, H. Zheng, H. Jin, L. Wang, M. Cao, Temperature- and thickness-dependent electrical conductivity of few-layer graphene and graphene nanosheets, Phys. Lett. A 379 (2015) 2245–2251.
[19] J. Tucek, P. Błonski, J. Ugolotti, A.K. Swain, T. Enoki, R. Zboril, Emerging chemical strategies for imprinting magnetism in graphene and related 2D materials for spintronic and biomedical applications, Chem. Soc. Rev. 47 (2018) 3899–3990.
[20] H.S.S. Ramakrishna Matte, K.S. Subrahmanyam, C.N.R. Rao, Novel magnetic properties of graphene: presence of both ferromagnetic and antiferromagnetic features and other aspects, J. Phys. Chem. C 113 (2009) 9982–9985.
[21] T. Enoki, Y. Kobayashi, K. Fukui, Electronic structures of graphene edges and nanographene, Int. ReV. Phys. Chem. 26 (2007) 609–645.
[22] T. Enoki, Y. Kobayashi, Magnetic nanographite: an approach to molecular magnetism, J. Mater. Chem. 15 (2005) 3999–4002.
[23] R. Saito, G. Dresselhaus, M.S. Dresselhaus, Physical Properties of Carbon Nanotubes, Imperial College Press (Knovel Library), London, 1998.

[24] V.W. Brar, R. Decker, H.M. Solowan, Y. Wang, L. Maserati, K.T. Chan, H. Lee, C.O. Girit, A. Zettl, S.G. Louie, M.L. Cohen, M.F. Crommie, Gate-controlled ionization and screening of cobalt adatoms on a graphene surface, Nat. Phys. 7 (2011) 43–47.
[25] N. Kaur, K. Pal, Enhanced magnetic properties of cobalt-doped graphene nanoribbons, Appl. Phys. A 123 (2017) 259–266.
[26] Y. Wang, Y. Huang, Y. Song, X. Zhang, Y. Ma, J. Liang, Y. Chen, Room-temperature ferromagnetism of graphene, Nano Lett. 9 (2009) 220–224.
[27] T. Abtew, B. Shih, S. Banerjee, P. Zhang, Graphene–ferromagnet interfaces: hybridization, magnetization and charge transfer, Nanoscale 5 (2013) 1902–1909.
[28] P. Hota, A.J. Akhtar, S. Bhattacharya, M. Miah, S.K. Saha, Ferromagnetism in graphene due to charge transfer from atomic Co to graphene, Appl. Phys. Lett. 111 (2017) 042402.
[29] F.V. Tikhonenko, D.W. Horsell, R.V. Gorbachev, A.K. Savchenko, Weak localization in graphene flakes, Phys. Rev. Lett. 100 (2008) 056802.
[30] S.V. Morozov, K.S. Novoselov, M.I. Katsnelson, F. Schedin, L.A. Ponomarenko, D. Jiang, A.K. Geim, Strong suppression of weak localization in graphene, Phys. Rev. Lett. 97 (2006) 016801.
[31] B. Balarajua, S. Kaleemullab, C. Krishnamoorthic, Structural and magnetic properties of NiO-MnO2 nanocomposites prepared by mechanical milling, J. Magnet. Magnet. Mater. 464 (2018) 36–43.
[32] A. Zelenakova, J. Kovac, V. Zelenak, Exchange bias in iron-oxide particles nanocasted in periodic porous silica, Acta Phys. Polon. Ser. A 115 (2009) 357–359.
[33] P. Mallick, C. Rath, A. Rath, A. Banerjee, N.C. Mishra, Antiferro to superparamagnetic transition on Mn doping in NiO, Solid State Commun. 150 (2010) 1342–1345.
[34] S.D. Tiwari, K.P. Rajeev, Signatures of spin-glass freezing in NiO nanoparticles, Phys. Rev. B 72 (2005) 104433.
[35] S. Lin, D.F. Shao, J.C. Lin, L. Zu, X.C. Kan, B.S. Wang, Y.N. Huang, W.H. Song, W.J. Lu, P. Tong, Y.P. Sun, Spin-glass behavior and zero-field-cooled exchange bias in a Cr-based antiperovskite compound $PdNCr_3$, J. Mater. Chem. C 3 (2015) 5683–5696.
[36] V.N. Matveev, V.I. Levashov, O.V. Kononenko, V.T. Volkov, Large positive magnetoresistance of graphene at room temperature in magnetic fields up to 0.5 T, Scrip. Mater. 147 (2018) 37–39.
[37] Y. Wang, M. Jaiswal, M. Lin, S. Saha, B. Ozyilmaz, K.P. Loh, Electronic properties of nanodiamond decorated graphene, ACS Nano 6 (2012) 1018–1025.
[38] S. Bhattacharya, D. Dinda, E.M. Kumar, R. Thapa, S.K. Saha, Charge transfer induced ferromagnetism and anomalous temperature increment of coercivity in ultrathin α-Fe_2O_3 decorated graphene 2D nanostructures, J. Appl. Phys. 125 (2019) 233904.
[39] A.L. Lin, H. Peng, Z. Liu, T. Wu, C. Su, K.P. Loh, W. Ariando, A.T.S.W. Chen, Room Temperature magnetic graphene oxide- iron oxide nanocomposite based magnetoresistive random access memory devices via spin-dependent trapping of electrons, Small 10 (2014) 1945–1952.
[40] L. Ovsiienko, L. Matzui, I. Berkutov, I. Mirzoiev, T. Len, Y. Prylutskyy, O. Prokopov, U. Ritter, Magnetoresistance of graphite intercalated with cobalt, J. Mater. Sci. 53 (2018) 716–726.
[41] C. Cai, J. Chen, Electronic transport properties of Co cluster decorated graphene, Chin. Phys. B 067304 (2018).
[42] S.C. Bodepudi, P. Singh, S. Pramanik, Giant current-perpendicular-to-plane magnetoresistance in multilayer graphene as grown on nickel, Nano Lett. 14 (2014) 2233–2241.
[43] Y. Hu, M. Ji, J. Peng, W. Qiu, M. Pan, J. Zhao, Y. Yao, C. Han, J. Hu, L. Pan, W. Tiana, D. Chen, Q. Zhang, P. Li, Anomalous temperature dependence of the magnetoresistance in vertical Ni/graphene/Ni junctions, J. Magnet. Magnet. Mater. 487 (2019) 165317.
[44] J. Kelber, P. Dowben, Coherent Spin Field Effect Transistor, US. Patent, Patent No. :US9,620,654B2 (2017).